

# Constraining the mass and redshift evolution of the hydrostatic mass bias using the gas mass fraction in galaxy clusters

R. Wicker<sup>1,\*</sup>, M. Douspis<sup>1</sup>, L. Salvati<sup>1</sup>, and N. Aghanim<sup>1</sup>

<sup>1</sup>Université Paris-Saclay, CNRS, Institut d'Astrophysique Spatiale, 91405 Orsay, France

**Abstract.** The gas mass fraction in galaxy clusters is a quantity which can be used as a robust cosmological probe. It is however subject to various effects from the baryonic physics inside galaxy clusters, which may bias the obtained cosmological constraints. Among different aspects of the baryonic physics, in these proceedings we focus on the impact of the hydrostatic equilibrium assumption. From X-ray measurements of cluster gas fraction in the *Planck*-ESZ sample, we analyse the hydrostatic mass bias  $B$ , constraining a possible mass and redshift evolution of this quantity and its impact on the cosmological constraints. We show a degeneracy between the redshift dependence of the bias and cosmological parameters. In particular we find a  $3.8\sigma$  evidence for a redshift dependence of the bias when assuming a *Planck* prior on  $\Omega_m$ . On the other hand, assuming a constant mass bias would lead to the extreme large value of  $\Omega_m > 0.860$ . We however show these results to be depending on the mass and redshift selections inside the main sample. Nevertheless, in all the analyses we find a value for the amplitude of the bias that is consistent with  $B \sim 0.8$ , as expected from hydrodynamical simulations and local measurements, but still in tension with the low value of  $B \sim 0.6$  derived from the combination of cosmic microwave background primary anisotropies with cluster number counts. We also discuss cosmological constraints obtained from gas fraction data, combined with other probes like cluster number counts.

## 1 Introduction

Clusters of galaxies are generally considered to be the most massive virialized structures in the universe, and as such are considered as standard cosmological probes [1, 2]. In particular, the mass fraction of gas enclosed in a particular radius is a robust probe for cosmological parameters, as it is considered to be a good proxy for the universal baryon fraction  $\Omega_b/\Omega_m$  [3, 4]. In addition, the cosmological use of the gas mass fraction relies solely on redshift, gas mass and total mass measurements. However, galaxy clusters are the host of a variety of astrophysical effects originating from baryonic physics, which will affect the total mass estimations. In particular, when estimating cluster masses from X-rays or combined X-rays and Sunyaev-Zel'dovich (SZ, [5]) observations, the standard assumption is to consider that all the gas is at hydrostatic equilibrium. These ideal conditions will however be departed from due to baryonic effects among which shocks, cosmic rays, magnetic fields, or other sources

\*e-mail: [raphael.wicker@universite-paris-saclay.fr](mailto:raphael.wicker@universite-paris-saclay.fr)

of non-thermal pressure support [6–11], biasing the total mass estimations. This *hydrostatic mass bias*,  $B = M_{HE}/M_{tot}$  where  $M_{HE}$  is the total mass estimated under hydrostatic equilibrium, has been constrained using several direct [12–16] or indirect [17–20] methods, giving sometimes contradictory results, with some of them showing a possible evolution of the bias with mass and redshift. The purpose of this work is to use the gas mass fraction of clusters to provide an independent direct constraint on the mass bias  $B$ , and to investigate its possible evolution with mass and redshift. In particular, we aim at investigating how an evolution of the bias would affect the cosmological constraints derived from the cluster gas fraction. This work is also described in detail in [21]. Throughout these proceedings, we assume a reference cosmology with  $H_0 = 70 \text{ km s}^{-1} \text{ Mpc}^{-1}$ ,  $\Omega_m = 0.3$ , and  $\Omega_\Lambda = 0.7$ .

## 2 Data

In this work we used the gas mass and hydrostatic mass measurements of 120 clusters from the *Planck*-ESZ sample [22], taken at  $R_{500}$ . The masses were obtained in [23], using *XMM-Newton* data, by integrating the gas density profiles to obtain the gas mass, and solving the hydrostatic equilibrium equation for the hydrostatic mass. From the gas and hydrostatic masses, we computed the observed gas fractions  $f_{gas,obs} = M_{gas}/M_{HE}$ , and analysed their distribution depending on mass and redshift (see Figure 1 below). The clusters in the sample span the range [0.059; 0.546] in redshift and [0.06; 0.20] in gas fractions, with hydrostatic masses ranging from  $2.22 \times 10^{14} M_\odot$  and  $1.75 \times 10^{15} M_\odot$ . Note that the gas fraction sample used in this analysis has been made public <sup>1</sup>.

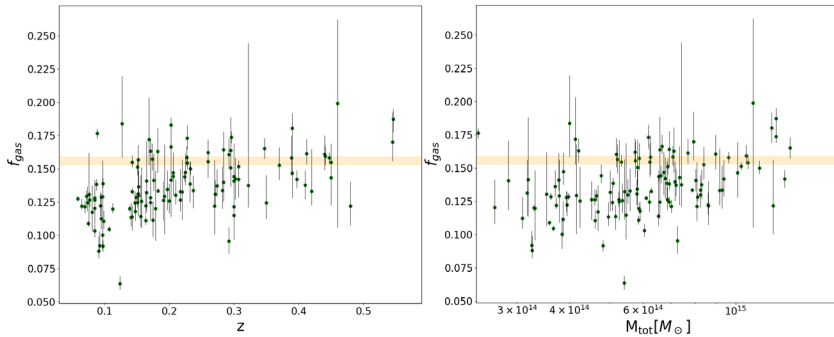


**Figure 1.** Observed gas fraction in the *Planck*-ESZ sample, compared to the universal baryon fraction  $\Omega_b/\Omega_m = 0.156 \pm 0.003$  from [20].

## 3 Theoretical modelling

The general assumption when using the cluster gas fraction as a cosmological probe is that this quantity is a direct proxy to the universal baryon fraction, so that  $f_{gas} \propto \Omega_b/\Omega_m$ . However, several additional astrophysical, instrumental, and cosmological contributions need to be taken into account when studying the gas fraction from X-ray data, including but not limited to the hydrostatic mass bias  $B(z, M)$ . The full theoretical model for the gas fraction we expect to observe is given by [3] :

$$f_{gas}(z, M) = K \times \frac{\Upsilon(z, M)}{B(z, M)} \times A(z) \times \frac{\Omega_b}{\Omega_m} \times \left( \frac{D_A^{ref}(z)}{D_A(z)} \right)^{3/2} - f_*, \quad (1)$$

<sup>1</sup>Planck-ESZ gas fraction sample available at the CDS via anonymous ftp to cdsarc.cds.unistra.fr (130.79.128.5) or via <https://cdsarc.cds.unistra.fr/viz-bin/cat/J/A+A/674/A48>.

where  $K$  accounts for a possible instrumental calibration bias,  $A(z)$  is an angular correction accounting for all the mass measurements being performed in a reference cosmology,  $D_A(z)$  is the angular diameter distance and  $f_*$  is the stellar mass fraction of clusters. Throughout these proceedings, any quantity noted  $X^{ref}$  is said quantity computed in the reference cosmology defined in Sect. 1, while the quantity  $X$  is the "test" quantity, computed in a test cosmology. We additionally consider an intrinsic scatter  $\sigma_f$ , which we treat as a free parameter and which appears in the computation of the complete likelihood.

The factor  $\Upsilon(z, M)$  is the so called "baryon depletion factor", which accounts for how baryons in clusters are depleted with respect to the universal value. As both the mass bias and the depletion may trigger an evolution of the gas fraction with mass and redshift, an accurate understanding of this latter quantity is necessary. From hydrodynamical simulations, robust constraints can be put on  $\Upsilon$ , and we take  $\Upsilon = 0.85 \pm 0.03$  from [24]. Following the results of simulation works in our mass range (discussed in [25]), we consider the depletion factor to be constant. On the other hand, we allow the mass bias to vary with mass and redshift, and parameterize it following a simple power law:

$$B(z, M) = B_0 \left( \frac{M}{\langle M \rangle} \right)^\alpha \left( \frac{1+z}{\langle 1+z \rangle} \right)^\beta. \quad (2)$$

In a first step of the analysis, we consider three different scenarios to test the effect of assuming a constant or a varying bias on the cosmological constraints which can be inferred from our gas fraction data:

- **CB scenario:** We consider a constant bias, i.e.  $(\alpha, \beta) = (0, 0)$  and only the amplitude  $B_0$  is left free to vary.
- **VB scenario:** All three bias parameters  $(B_0, \alpha, \beta)$  are left free to vary.
- **VB +  $\Omega_m$  scenario:** All three bias parameters  $(B_0, \alpha, \beta)$  are left free to vary, and a prior from [20] is set on the matter density  $\Omega_m = 0.315 \pm 0.007$ .

In this step of the analysis, we consider a prior on the total value of the bias at a pivot mass and redshift, from [26]:

$$B(z = 0.189, M = 6.24 \times 10^{14} M_\odot) = 0.84 \pm 0.04. \quad (3)$$

The purpose of this prior is to break the degeneracy existing between  $B$  and  $\Omega_b/\Omega_m$ .

As different works focused on constraining the mass bias and its evolution have found results which may depend on the considered sample (e.g. [16]), we check for a possible sample dependence of our results in a second step of the analysis. In particular, in addition to the full sample we define two subsamples in which we will compare the retrieved trends of the mass bias:

- **Low  $M_z$  subsample:** All clusters below  $z = 0.2$  and below the median mass of the sample  $M_{med,ESZ} = 5.89 \times 10^{14} M_\odot$  fall within this subsample. This subsample contains 47 clusters.
- **High  $M_z$  subsample:** All clusters above  $z = 0.2$  and above the median mass of the sample  $M_{med,ESZ} = 5.89 \times 10^{14} M_\odot$  fall within this subsample. This subsample contains 45 clusters.

The redshift cut of  $z = 0.2$  was selected to mimic the selection of several other weak lensing works aimed at constraining the mass bias (see e.g. [12, 14, 15]). In this step of the analysis, as we are focusing on the mass and redshift trends of the bias and not so much on their degeneracies with cosmological parameters, we put a prior on  $\Omega_b/\Omega_m = 0.156 \pm 0.003$  from [20], in order to be able to remove the prior on the total value of the bias. The complete set of priors we consider for the two steps of the analysis is given in Table 1 below.

**Table 1.** Set of priors used in the analysis. A prior noted  $\mathcal{U}(l, u)$  is a uniform prior of lower bound  $l$  and upper bound  $u$ , a prior noted  $\mathcal{N}(\mu, \sigma)$  is a gaussian prior of mean  $\mu$  and standard deviation  $\sigma$ .  $z_{piv}$  and  $M_{piv}$  are the pivot redshift and mass at which the prior on the bias is applied, given in Eq.3. In the study of sample dependence, we do not consider any prior on the total value of the bias at a pivot mass and redshift.

|                       | Bias evolution study                                                                 | Sample dependence of the results |
|-----------------------|--------------------------------------------------------------------------------------|----------------------------------|
| Parameter             | Prior                                                                                | Prior                            |
| $B_0$                 | $\mathcal{U}(0.3, 1.7)$                                                              | $\mathcal{U}(0.3, 1.7)$          |
| $B(z_{piv}, M_{piv})$ | $\mathcal{N}(0.84, 0.04)$                                                            | –                                |
| $f_*$                 | $\mathcal{N}(0.015, 0.005)$                                                          | $\mathcal{N}(0.015, 0.005)$      |
| $\Upsilon_0$          | $\mathcal{N}(0.85, 0.03)$                                                            | $\mathcal{N}(0.85, 0.03)$        |
| $K$                   | $\mathcal{N}(1, 0.1)$                                                                | $\mathcal{N}(1, 0.1)$            |
| $\sigma_f$            | $\mathcal{U}(0, 1)$                                                                  | $\mathcal{U}(0, 1)$              |
| $h$                   | $\mathcal{N}(0.674, 0.005)$                                                          | $\mathcal{N}(0.674, 0.005)$      |
| $\Omega_b/\Omega_m$   | $\mathcal{U}(0.05, 0.3)$                                                             | $\mathcal{N}(0.156, 0.003)$      |
| $\Omega_m$            | $\mathcal{U}(0.01, 1)$ (CB, VB) or<br>$\mathcal{N}(0.315, 0.007)$ (VB + $\Omega_m$ ) | $\mathcal{N}(0.315, 0.007)$      |
| $\alpha$              | Fixed at 0 (CB) or $\mathcal{U}(-2, 2)$ (VB, VB + $\Omega_m$ )                       | $\mathcal{U}(-2, 2)$             |
| $\beta$               | Fixed at 0 (CB) or $\mathcal{U}(-2, 2)$ (VB, VB + $\Omega_m$ )                       | $\mathcal{U}(-2, 2)$             |

## 4 Results

### 4.1 Study of the bias evolution

We show in Figure 2 the results of the first part of the analysis, focusing on investigating the trends of the mass bias and its degeneracies with cosmological parameters.

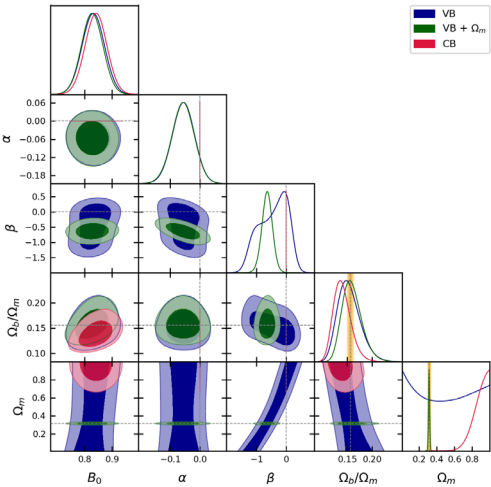


**Figure 2.** 1D and 2D posterior distributions for the CB, VB, and VB +  $\Omega_m$  scenarios. The contours mark the 68% and 95% confidence level (c.l.). The gray dashed lines highlight reference values for  $(\alpha, \beta, \Omega_b/\Omega_m, \Omega_m) = (0, 0, 0.156, 0.315)$ . The orange bands mark the values from [20] for  $\Omega_b/\Omega_m$  and  $\Omega_m$  at  $2\sigma$  c.l.

We show in particular that a strong degeneracy exists between the matter density  $\Omega_m$  and the redshift evolution of the bias  $\beta$ , highlighted in the posterior distributions for the VB scenario (blue contours). Under the effect of this degeneracy, when assuming a constant bias in the CB scenario the matter density is pushed to high values, with  $\Omega_m > 0.860$ . This value is

in strong disagreement with all other cosmological studies and is completely aberrant. When imposing a *Planck* prior on the matter density in the VB +  $\Omega_m$  scenario, the degeneracy between  $\Omega_m$  and  $\beta$  leads the latter away from 0 at  $3.8\sigma$ , with  $\beta = -0.64 \pm 0.18$ . This value of  $\beta < 0$  would mean that at higher redshifts, the mass measurements would be more biased than at lower redshifts.

In all scenarios however, our results are in agreement within  $2\sigma$  with a mass-independent bias, with  $\alpha = -0.057 \pm 0.038$ , and the amplitude  $B_0$  is in agreement with other direct constraints on the bias, with  $B_0 = 0.832 \pm 0.041$  in the VB scenario. However, these result are in disagreement with the indirect measurements from [17–19], pointing closer to  $B = 0.62 \pm 0.03$ .

## 4.2 Sample dependence of the results

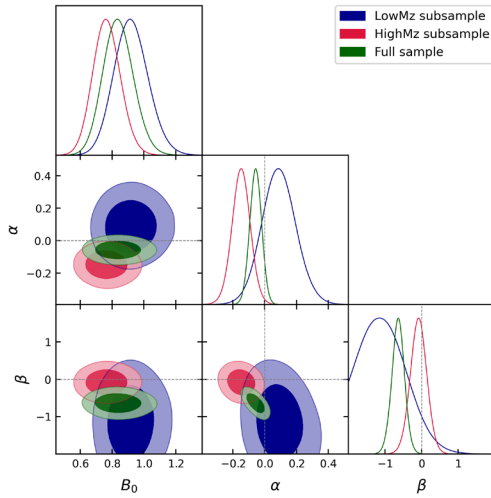


**Figure 3.** 1D and 2D posterior distributions for the bias parameters in the three mass and redshift selected samples. The levels of the contours mark the 68% and 95% confidence levels. The gray dashed lines mark the reference values  $(\alpha, \beta) = (0, 0)$ .

We show in Figure 3 the comparison of the trends obtained in the VB +  $\Omega_m$  scenario for the full sample, and the two mass and redshift selected subsamples. We show that in all subsamples, the value of the amplitude of the bias is agreeing well around  $B \sim 0.8$ , in agreement with other direct measurements, with  $B_{0,full} = 0.840 \pm 0.095$ ,  $B_{0,LowMz} = 0.92^{+0.10}_{-0.11}$ , and  $B_{0,HighMz} = 0.767 \pm 0.086$ , but still in disagreement with indirect measurements.

However, when focusing on the trends of the mass bias, discrepancies appear between the different subsamples. Indeed, with  $(\alpha, \beta) = (0.09 \pm 0.11, -0.995^{+0.44}_{-0.77})$ , the trends exhibited in the *Low Mz* subsample are in agreement with the trends found in the full sample, with a mass-independent bias but a non-zero redshift evolution, and masses which are more biased at higher redshifts. On the other end of the mass-redshift plane, however, in the *High Mz* subsample, the trends seem to exhibit the opposite behaviour. Indeed, with  $(\alpha, \beta) = (-0.149 \pm 0.58, -0.08 \pm 0.23)$  the preferred scenario is that of a redshift-independent bias, yet with evidence for a mass evolution, where more massive clusters have more biased mass estimates than less massive clusters. This highlights a strongly sample dependent behaviour, which had been noted in other works using weak lensing data or SZ number counts [15, 16, 26].

## 5 Conclusion

With this work, we have shown that the gas mass fraction of galaxy clusters can be used as a robust probe for the hydrostatic mass bias and its evolution with mass and redshift. In

particular, we have shown the strong degeneracy that exists between the evolution of the bias with redshift and cosmological parameters, among which the matter density  $\Omega_m$ . This degeneracy leads to unrealistic constraints on the matter density when considering a constant bias. Reversely, when assuming a *Planck* prior on  $\Omega_m$ , we find a redshift-dependent bias with  $\beta = -0.64 \pm 0.18$ . We however show that these results are strongly dependent on the considered sample, with the trends of the mass bias depending on selection of clusters depending on mass and redshift. It is important to note that limitations may affect this study, among which are assumptions on the baryon depletion factor, or other effects which may trigger a mass and redshift evolution of the gas fraction, for instance deviations from self-similarity. All these effects are discussed in detail in the complete paper [21].

In a work in progress by Wicker *et al in prep.*, this sensitivity of the gas fraction to the hydrostatic mass bias is put to use in a cosmological study, combined with galaxy cluster number counts. Indeed, galaxy cluster number counts constitute a robust cosmological probe allowing for tight constraints on cosmological parameters. However the results from number counts are fully dependent on the mass calibration, and thus on the level of mass bias. Combining number counts and gas fraction data may allow to benefit both from the strong cosmological sensitivity of number counts, and the sensitivity of the gas fraction to astrophysical effects, to obtain cosmological constraints which are independent on any prior on the mass bias.

## References

- [1] S.D.M. White *et al.*, *Nature* **366**, 429 (1993)
- [2] S. W. Allen *et al.*, *Annual Rev. of Astron. Astrophys.* **49**, 409 (2011)
- [3] S. W. Allen *et al.*, *MNRAS* **383**, 879 (2008)
- [4] S. Borgani, A. Kravtsov, *Adv. Sci. Letters* **4**, 204 (2011)
- [5] R. A. Sunyaev, Y.B. Zeldovich, *Comments on Astrophys. and Space Phys.* **4**, 173 (1972)
- [6] E. Lau *et al.*, *ApJ* **705**, 1129 (2009)
- [7] F. Vazza *et al.*, *Astron. Astrophys.* **504**, 33 (2009)
- [8] N. Battaglia *et al.*, *ApJ* **758**, 74 (2012)
- [9] K. Nelson *et al.*, *ApJ* **792**, 25 (2014)
- [10] X. Shi *et al.*, *MNRAS* **448**, 1020 (2015)
- [11] V. Biffi *et al.*, *ApJ* **827**, 112 (2016)
- [12] A. von der Linden *et al.*, *MNRAS* **443**, 1973 (2014)
- [13] H. Hoekstra *et al.*, *MNRAS* **449**, 685 (2015)
- [14] N. Okabe, G. Smith, *MNRAS* **461**, 3794 (2016)
- [15] M. Sereno, S. Ettori, *MNRAS* **468**, 3322 (2017)
- [16] L. Salvati *et al.*, *Astron. Astrophys.* **626**, A27 (2019)
- [17] Planck Collab. *et al.*, *Astron. Astrophys.* **571**, A20 (2014)
- [18] Planck Collab. *et al.*, *Astron. Astrophys.* **594**, A24 (2016)
- [19] L. Salvati *et al.*, *Astron. Astrophys.* **614**, A13 (2018)
- [20] Planck Collab. *et al.*, *Astron. Astrophys.* **641**, A6 (2020)
- [21] R. Wicker *et al.*, *Astron. Astrophys.* **674**, A48 (2023)
- [22] Planck Collab. *et al.*, *Astron. Astrophys.* **536**, A8 (2011)
- [23] L. Lovisari *et al.*, *ApJ* **892**, 102 (2020)
- [24] S. Planelles *et al.*, *MNRAS* **431**, 1487 (2013)
- [25] D. Eckert *et al.*, *Astron. Astrophys.* **621**, A40 (2019)
- [26] R. Herbonnet *et al.*, *MNRAS* **497**, 4684 (2020)